Full Paper Transactions, SMiRT 28
Toronto, Canada, August 10-15, 2025

GROUND MOTION SELECTION FOR BASE ISOLATED STRUCTURES AND COMPONENTS

Soumitra Chatterji[1], Philippe L.A. Renault[2], Felix Weber[3]

[1] M.Sc., RWTH Aachen University, Aachen, Germany (chatterji@lbb.rwth-aachne.de)
[2] Dr.-Ing., SDA-engineering GmbH, Herzogenrath, Germany (renault@sda-engineering.de)
[3] Dr.-Ing., Maurer Switzerland GmbH, Pfaffhausen, Switzerland (F.Weber@maurer.eu)

ABSTRACT

Today, dynamic analysis for relevant SSCs (Structures, Systems & Components) under seismic loads are performed based on time history analyses to study their response as realistically as possible. Depending on the case, site-specific seismic hazard analyses results in form of a UHS (Uniform Hazard Spectrum) or a code-based response spectrum are available as a starting point. An increasing interest in base isolation for SMR (Small Modular Reactors) has manifested to standardize the design and thus, to envelope as many seismic hazard conditions as possible and keep the standard design identical. When designing or analysing existing SSCs considering base isolation, the choice of time histories to be used for the analysis becomes relevant. As the base isolation filters out to a certain degree all motions above the natural frequency of the device, special attention should be paid to the properties of the selected time histories at and around the natural frequency (or isolation period). In this paper, the different approaches used in practice are compared for a simple single degree of freedom system in order to draw conclusions on the differences in isolator responses, even if the statistical properties of the ground motions in terms of agreement with the target response spectra are almost identical.

INTRODUCTION

The recent M7.7 Sagaing region earthquake in Myanmar (2025) and other recent devastating events like the Kahramanmaras earthquake in Turkey (2023) and Noto Peninsula earthquake (2024) in Japan have underscored the vulnerability of critical infrastructure to seismic events. These recent disasters emphasize the urgent need to enhance earthquake resilience in critical facilities, through robust analysis and design techniques that can prevent catastrophic failures in essential structures. In this context, ground motion selection has become a pivotal role for non-linear time history analysis (NLTHA) of structures. The chosen earthquake time histories must accurately represent the seismic hazard, intensity and frequency content expected at the considered site, since the structural response strongly depends on the input ground motions. Studies showed that using hazard-consistent records leads to more reliable predictions of structural performance than arbitrary or envelope-based approaches (Bassman et al., 2022).

One earthquake resilience strategy gaining prominence is the use of seismic isolation. Base isolation protects a structure by inserting flexible or sliding bearings at its base, effectively decoupling the building and its equipment from the shaking ground. This design approach filters out the high intensity frequency components of the earthquake and shifts the overall structure's fundamental period to a much longer value, typically ≥ 3 seconds (IAEA, 2020). This results in the reduction of acceleration and force transmitted to the superstructure by increasing the displacements occurring in the isolation bearings. Lead–rubber bearings (LRBs) and curved surface sliders (CSSs) have proven to be efficient base isolators (Yaacoub et al., 2025). Some nuclear structures worldwide have been put on base isolators. For example, the Cruas NPP in France, the Koeberg NPP in South Africa, the fuel wet storage in Gösgen – Switzerland and the ITER fusion reactor in Cadarache France, and they have proven to work. In the framework of bringing Small Modular Reactors (SMR) to the market, there is growing interest in applying seismic isolation to nuclear installations and reactor technologies (IAEA, 2020). In principle, base isolation can be implemented in new nuclear power plants as well as retrofitted to certain existing safety relevant structures, providing additional protection for reactors, control rooms, and other critical systems. This approach aligns with the nuclear industry's goal of ensuring that vital systems remain functional even during beyond-design-basis earthquakes.

The design of seismically isolated structures for nuclear installations requires particular care in the selection of input ground motions. Base isolators, i.e. LRBs and CSSs exhibit nonlinear behaviour and can be sensitive to the characteristics of ground motion input. In particular, the predicted response of an isolator, especially the isolator displacement and consequently the base shear, can vary widely depending on the frequency content, duration, and amplitude of the earthquake record used. For instance, a near-fault ground motion containing a large velocity pulse may challenge the isolators with significantly larger displacement demands than a far-field motion of the same peak acceleration. Dicleli (2006) showed that the number and period of velocity pulses, as well as the magnitude and distance of the earthquake, strongly influence isolator response, making an accurate representation of expected ground motion crucial for correct design.

Given the significance of these issues, the paper focuses on the effects of ground motion selection techniques in NLTHA in the context of seismic analysis of seismic isolators. It discusses the state-of-the-art methods for selecting and scaling input motions and investigates how different selection strategies influence the engineering demand parameters (EDP) of a base-isolator.

METHODOLOGY

A CSS of type single was selected for nonlinear time history analysis (NLTHA). The isolator parameters were calibrated in LS-DYNA and validated against a previously conducted experimental study to ensure accurate representation of its hysteretic behaviour. Five target response spectra (UHS) were defined for the city of Istanbul, corresponding to different return period (RP) as 100 y, 200 y, 500 y, 1000 y and 2500 y obtained from the European Seismic Hazard Model (ESHM20) EFEHR website (Dancui et al. 2021). These spectra were linearly scaled to spectral acceleration values S_a of 0.05 g, 0.10 g, 0.15 g, 0.20 g, and 0.25 g at the effective period of the isolator T_{eff}. The used spectra are interpreted as deterministic design requirement in the context of this study. To assess the influence of ground motion selection techniques on the isolator displacement response, four distinct selection methods were employed: (i) database filtering, (ii) Mean Square Error (MSE) minimization, (iii) spectral matching, and (iv) conditional spectrum approach. For each target spectral acceleration level, 30 sets of unidirectional ground motion records were selected using each method, resulting in a comprehensive suite of inputs for probabilistic evaluation. The superstructure is modelled as one rigid mass. The overall NLTHA methodology is illustrated in Figure 1, where selected ground motion acceleration $\ddot{x}_g(t)$ are applied unidirectionally at the base of a CSS isolator.

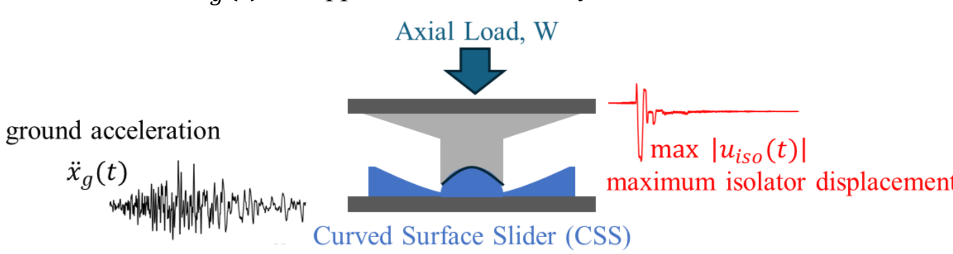

Figure 1. Application of selected ground acceleration and estimating the resulting maximum isolator displacement.

The engineering demand parameter (EDP) of interest – here maximum isolator displacement max $|u_{iso}(t)|$ is extracted from each analysis and compared for each approach.

MODELLING AND VALIDATION OF SINGLE CURVED SURFACE SLIDER (CSS)

The modelling and validation of the CSS in LS-DYNA was conducted by benchmarking against a hysteresis curve obtained from a prototype specimen tested under lateral displacements smaller than the design displacement. The physical tests followed the protocol defined in EN 15129 (2018), wherein a sine-wave displacement history is imposed with an initial intro-cycle (half-cycle with maximum velocity at zero displacement), followed by three full harmonic cycles and a final exit cycle. These cycles served as the reference for numerical model calibration. The parameters listed in the Table 1 were used in modelling and calibration of the numerical isolator model.

Table 1: Parameters of the single CSS used in modelling and calibration of isolator model in LS-DYNA

Parameter	Symbol	Value	Unit
Effective radius	R_{eff}	5.826	[m]
Axial load / Weight	W	4070	[kN]
Amplitude of max. displacement	D_{max}	192	[mm]
Dynamic friction coefficient	μ_{dyn}	0.077	[-]
Transition rate parameter	D	10	[s/m]
Pre-sliding stiffness	K_y	106.7	[kN/mm]
Dimensionless model constant	A	1	[-]
Dimensionless model constant	γ	0.1	[-]
Dimensionless model constant	β	0.9	[-]

Modelling and Calibration of CSS

CSS was modelled using MAT_197 (MAT_SEISMIC_ISOLATOR), which uses discrete beam element (ELEMENT_DISCRETE) with Material Type 6 for the nonlinear simulation of seismic isolation bearings (ANSYS, 2025). The calibration of the model was performed on transition rate (velocity multiplier in sliding friction equation) D and dimensionless constants of Bouc-Wen model of hysteresis i.e. A, γ and β. These dimensionless model constants govern the shape and energy dissipation characteristics of the hysteresis variable (Wen 1976, Park et al. 1986).

Validation of CSS

A unidirectional sinusoid loading was applied to CSS model with a frequency equal to the isolator's natural frequency f_{iso} of 0.21 Hz (corresponding to a period of 4.84 s) using Equation 1, and a peak displacement amplitude of 192 mm.

$$T_{iso} = 2\pi\sqrt{\frac{R_{eff}}{g}} = 2\pi\sqrt{\frac{5.826}{9.81}} = 4.84\ s \tag{1}$$

The resulting normalized horizontal force-displacement response (F/W-u_{iso}) is compared against the experimental results in Figure 2.

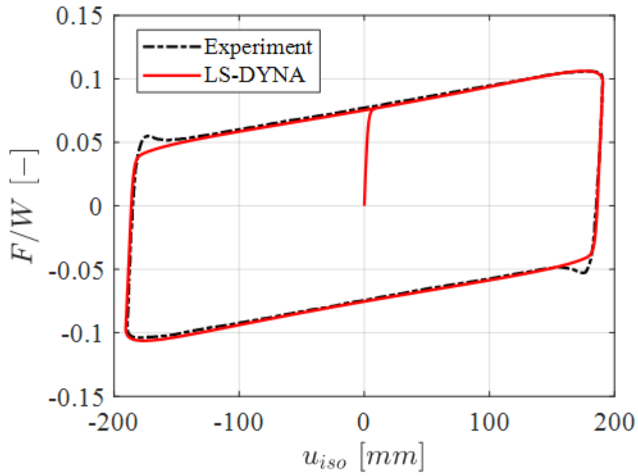

Figure 2. Comparison of single CSS hysteresis curve modelled in LS-DYNA with the experiment hysteresis curve

The effective time period T_{eff} of the single CSS system can be calculated as given in Equation 2:

$$T_{eff} = 2\pi\sqrt{\frac{W/g}{\frac{W}{R_{eff}}+\frac{\mu \cdot W}{D_{max}}}} = 2\pi\sqrt{\frac{4070/9.81}{\frac{4070}{5.826}+\frac{0.077 \cdot 4070}{0.192}}} = 2.65\ s \quad (2)$$

The comparison shows that numerical model captures the key hysteretic features of the experimental behaviour, including the characteristic energy dissipation and the elliptical shape of the frictional sliding loops. Overall, the numerical model closely reproduces the experimental response demonstrating good agreement between simulation and test results.

GROUND MOTION SELECTION

The disaggregation results of the seismic hazard assessment provide the governing magnitude and distance of the earthquake scenarios contributing the seismic hazard. The selection of ground motion records used for this comparison is based on recorded time histories available in NGA-West2 databases (Ancheta et al. 2014). The details of the ground motion selection procedures, scaling strategies, dataset sizes, and corresponding literature sources are summarized in Table 2 as described in the following:

Table 2: Selected ground motion sets for NLTHA

Selection Procedure	**Scaling**	**Set No. #**	**No. of Records**	**Reference**
Database Filtering	Unscaled	#1	30 x 5	Ancheta et al. (2014)
Minimize MSE	Scaled	#2	30 x 5	Ancheta et al. (2014)
Spectrum Matching	Scaled	#3	30 x 5	Al Atik and Abrahamson (2010)
Conditional Spectra	Scaled	#4	30 x 5	Baker and Lee (2018)

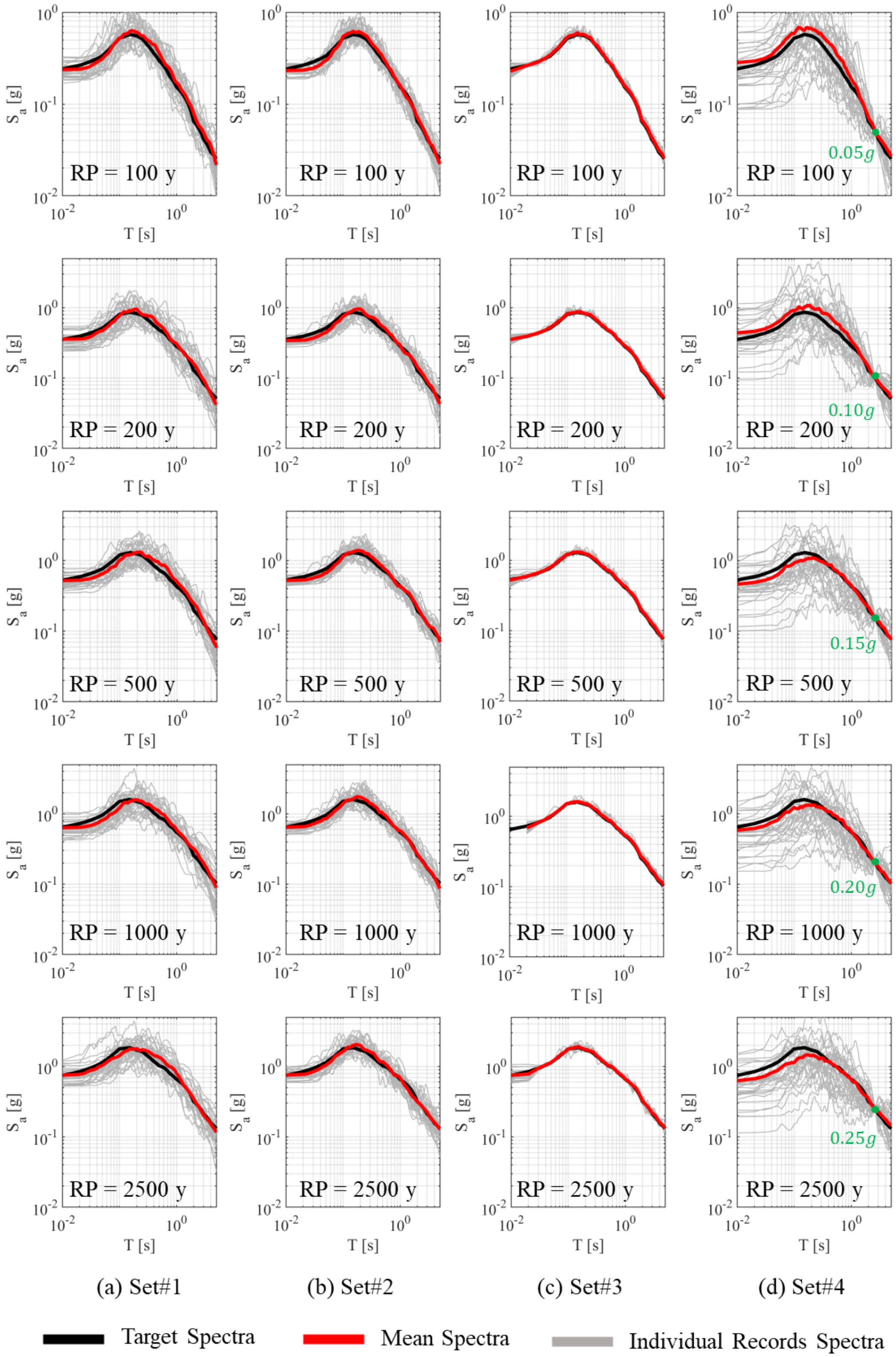

Figure 3. Acceleration response spectra (log-log representation) based on different ground motion selection technique (a) database filtering (b) minimize MSE (c) spectral matching (d) conditional spectra, with indication of the amplitude at the conditioning period.

Database Filtering

The database filtering approach was applied using the NGA-West2 ground motion database to assemble unscaled ground motion sets for each return period. For each return period, the corresponding target response spectra were first loaded. Ground motions were then searched based on moment magnitude (M_w) ranges that roughly reflect the dominant earthquake scenarios for each hazard level: RP100 (6.3–6.9), RP200 (6.5–7), RP500 (6.7–7.0), RP1000 (6.7–7.0), and RP2500 (6.8–10.0). Additionally, to ensure near-field characteristics, both Joyner-Boore distance (R_{jb}) and rupture distance (R_{rup}) were restricted to $\leq 50\ km$ across all return periods. This selection strategy is inherently approximate and relies on engineering judgment and iterative hit-and-trial filtering, with the objective of achieving a visual match between the mean spectrum of the selected ground motions and the target spectrum at each return period. This pragmatic method does not rely on formal optimization but is commonly used in early-phase studies due to its simplicity. The resulting unscaled ground motion sets referred to as **Set#1** and their spectral comparisons with the targets are illustrated in Figure 3a. Although significant variability in spectral acceleration is observed across the period range reflecting the natural dispersion of unscaled ground motions the mean response spectrum of the selected records demonstrates a satisfactory agreement with the target spectra.

Minimize MSE

The Minimize Mean Square Error (MSE) ground motion selection method was applied using the same magnitude and distance constraints as in the database filtering approach. However, in this case, scaling of ground motions or scale factors *SF* was restricted within a limited range (between 0.33 and 3.0) to mitigate potential bias introduced by excessive scaling. This method adjusts the scale of each ground motion to minimize the MSE between the scaled response spectrum ($SF \cdot S_a^{record}(T_i)$) and the target spectrum $S_a^{target}(T_i)$ across multiple period points T_i using weight points $w(T_i)$, following the formulation provided in Equation 3 and 4 (Ancheta et al. 2014).

$$MSE = \frac{\sum_i w(T_i) \cdot \left\{\ln\left[S_a^{target}(T_i)\right] - \ln\left[SF \cdot S_a^{record}(T_i)\right]\right\}^2}{\sum_i w(T_i)} \tag{3}$$

$$S_a^{target}(T_j) = SF \cdot S_a^{record}(T_j) \tag{4}$$

Equal weighting was assigned to period points ranging from 0.01s-10s, ensuring uniform spectral fitting across the entire period range. The resulting scaled ground motion sets, denoted as **Set #2**, and their spectral comparisons with the corresponding targets are shown in Figure 3b. In comparison to the database filtering approach, the variability in spectral acceleration of each record across the period range is notably reduced, and the mean spectrum exhibits a better match with the target spectra.

It is to be noted that the database filtering and MSE-based selection approaches was performed based on the square root of the sum of squares (SRSS) of the two horizontal components, H1 and H2 for spectral matching. Consequently, in the NLTHA, both components were applied independently to the isolator as separate input motions. The resulting EDP i.e., the maximum relative isolator displacement was computed as the SRSS of the individual responses to ensure consistency with spectral matching procedure.

Spectral Matching

The Spectral Matching procedure was employed to generate a suite of ground motions whose response spectra closely conform to the target spectra across the specified period range. This method was originally introduced by Lilhanand and Tseng (1988) and later refined by Al Atik and Abrahamson (2010). They developed a robust algorithm to modify the time history of recorded ground motions while preserving their nonstationary characteristics. In this study, the spectral matching was performed using the SeismoMatch software, which implements the RSPMatch algorithm based on wavelet transformation to iteratively adjust the acceleration time histories. To generate matched records, the horizontal components (H1 and H2) originally selected via the database filtering approach were used as input. These records were then modified to achieve a close fit to the target spectra associated with each return period. This process inherently alters both the frequency content and amplitude of each record to minimize the mismatch with the target spectra. The resulting spectrally matched ground motion sets are referred to as **Set#3**, and the spectral comparisons with the targets are presented in Figure 3c. As shown, each record exhibits a tight spectral fit, significantly reducing variability across the period range. Out of the H1–H2 pairs available for each return period, only a single horizontal component was selected for NTLHA specifically, the component with the lowest MSE relative to the target spectrum. In practice, since both H1 and H2 components typically exhibit similarly low MSE values after spectral matching, the distinction between them is minimal; however, for consistency, the component with the absolute lowest MSE was selected.

Conditional Spectra

The Conditional Spectrum (CS)-based ground motion selection was performed using the open-source MATLAB code developed by Baker and Lee (2018). This approach allows for the generation of ground motion suites that are consistent with a specific rupture scenario, while conditioning the spectra on a target period of interest. In this study, the conditioning period was selected as the effective period of the CSS isolator T_{eff} as given in Equation 2.

While source parameters - M_w and R_{jb} are commonly derived from hazard disaggregation results for a given site and return period, in this study these rupture scenario parameters were selected to minimize MSE between the mean spectrum of the selected records and the full target spectrum. Nevertheless, irrespective of the specific magnitude and distance values chosen, the CS method give appropriate scaling factor of that the selected ground motions will match the target spectrum at the conditioning period and bound of conditional variability. To reflect the high seismicity of Istanbul, rupture scenarios with $M_w > 7.0$ and $R_{jb} < 10$ km were prioritized to simulate large, near-field events. As necessary input, the average shear wave velocity was assumed as 800 m/s (corresponding to rock conditions in design codes), and the rupture region was specified as Turkey/China to maintain regional consistency. The resulting MSE values across the full period range were 0.01%, 0.04%, 0.91%, 1.25%, and 2.37% for RP100, RP200, RP500, RP1000, and RP2500 respectively. These record sets are referred to as **Set#4**, and their spectral comparisons with the targets are shown in Figure 3d. Figure 3d further illustrates that the mean response spectra of the selected records exhibit a strong agreement with the target spectra particularly in the long-period range (beyond 1 s). But it can also be noted that for RP100 and RP200 the mean of the selected ground motions is above the target spectra and thus more conservative, while it is significant lower at the higher return periods.

RESULTS AND DISCUSSION

Multi-stripe plots in Figure 4 shows how different ground motion selection methods influence the distribution of isolator displacement responses as $S_a(T_{eff})$ increases. The Sa levels represent the investigated RP100 to RP2500 respectively. The plot also shows the response scatter, central trend alignment (mean and median).

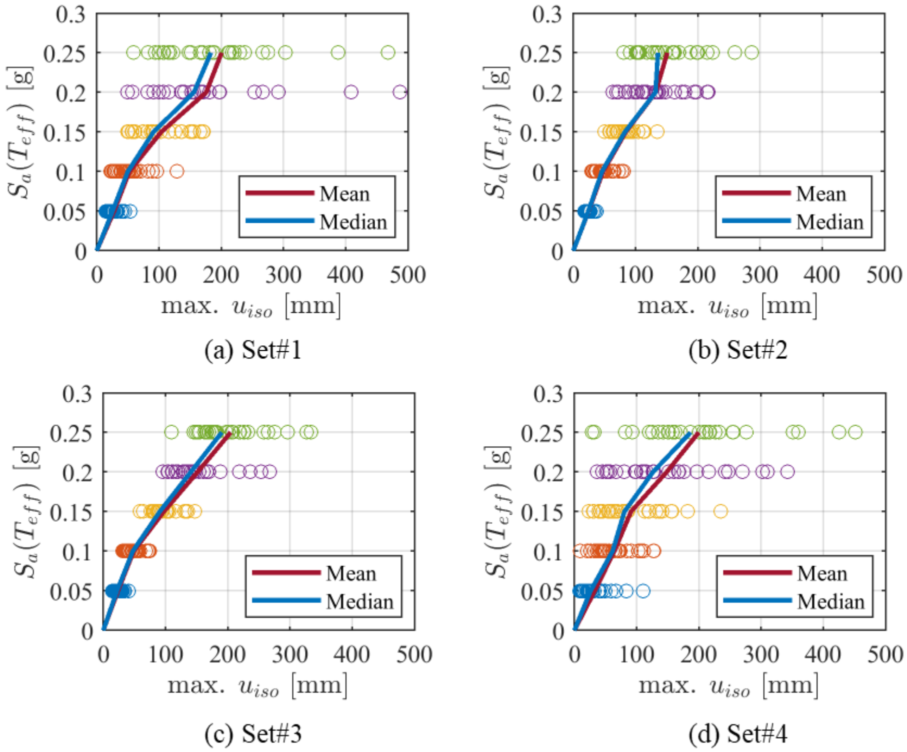

Figure 4. Multi-stripe plot of maximum isolator displacement of each record per target intensity measure with their corresponding mean and median using (a) database filtering (b) minimize MSE (c) spectral matching (d) conditional spectra procedure

Table 3 also presents the mean, median, standard deviation in *mm* and dispersion (using natural log) of isolator displacement responses across all different return period associated with each ground motion selection method.

Table 3: Mean μ, median $\bar{x}$, standard deviation σ, and dispersion β of CSS maximum isolator displacements across different return periods

Selection Procedure	**Parameter**	**100y**	**200y**	**500y**	**1000y**	**2500y**
#1 Database Filtering	μ	27.89	52.47	103.67	175.94	200.65
	$\bar{x}$	25.53	50.03	91.24	156.19	183.56
	σ	8.99	22.83	39.21	100.28	103.81
	β	0.31	0.41	0.40	0.54	0.50
#2 Minimize MSE	μ	24.61	47.84	84.41	132.35	151.05
	$\bar{x}$	24.27	46.06	82.96	132.15	136.08
	σ	4.63	13.43	21.12	42.28	49.96
	β	0.18	0.27	0.25	0.34	0.32
#3 Spectral Matching	μ	23.70	48.83	97.39	151.69	204.86
	$\bar{x}$	22.17	47.45	90.89	140.80	190.50

	σ	6.36	11.76	22.43	46.39	53.05
	β	0.26	0.24	0.23	0.28	0.25
#4 Conditional Spectra	μ	32.79	64.18	91.10	148.39	199.85
	$\bar{x}$	26.15	61.44	80.48	126.40	186.80
	σ	22.94	30.83	51.36	83.02	99.83
	β	0.65	0.59	0.61	0.60	0.63

In case of *database filtering selection* **(Set#1)**, the displacement response variability (Figure 4a) is high (not the highest) as expected at each intensity stripe (individual record responses shown as dots) and are widely scattered. This widespread arises from the diverse spectral shapes of the natural records since they are not optimized to a common spectrum. The mean/median trendline is also not smooth or consistent due to the high scatter. The trendline diverges at higher intensities exhibits some outliers (individual dots well far from the mean/median) reflecting that certain unfiltered records can cause exceptionally large isolator displacements.

For the *minimize MSE selection* **(Set#2)**, Figure 4b shows reduced scatter relative to database filtering i.e. the points cluster more tightly at each intensity level. The median/mean trendline are well-aligned and smooth with symmetrical around the central value. This suggests that no extreme outlier is heavily skewing the response except at the RP of 2500y. The only drawback is that it does not capture the full variability of possible spectra. By focusing on average fit, it might under-represent the range of spectral shapes that could occur for an expected S_a. Thus, the dispersion in responses while lower than Set#1, might also be artificially low relative to true hazard variability. Overall, MSE-based selection achieves a more stable and reliable median and it limits outliers but may fail to account true record-to-record variability.

In this study, *spectral matching-based selection* (**Set#3**) stands out with the tightest clustering of points with the minimum variability. The mean and median trendline is also extremely smooth and identical (virtually no skew) in Figure 4c. Outliers are absent i.e. no displacement value from the single record deviates far from the pack due to eliminated spectrum-to-spectrum differences. It exhibits "*nearly vanishing dispersion*" in response spectra and thus in structural responses (Manfredi et al. 2022). The dispersion β is among the lowest of approx. 0.25 and stable across increasing intensity level (Figure 5b). However, the lack of variability is a double-edged sword. While it simplifies interpretation, it fails to capture the natural variability of earthquake records i.e. real earthquakes at the same $S_a(T_{eff})$ can produce a range of response. Therefore, a suite with zero spectral variability might give a false sense of certainty when not considering the fractiles of the Uniform Hazard Spectrum. Another concern is potential bias from the overly conservative UHS target spectrum. In this case spectral matching will consistently overpredict isolator displacements relative to what the true hazard would median-wise demand. Nevertheless, spectral matching alters records (changing phase content, duration, etc.) which affect response in ways not captured by spectral shape alone. Thus, while Set#3 yields the least variability and most stable mean/median trend, it does not transport the variability of the UHS which needs to be considered additionally depending on the application purpose.

Conditional spectra-based selection (**Set#4**) yielded highest dispersion of approx. 0.6. Figure 4d shows a widest spread of isolator displacements definitely more than Set#2 and Set#3. For example, at a spectral acceleration $S_a(T_{eff})$ of 0.25g the isolator displacement ranged from 28 mm to 451 mm. However, the alignment of mean and median trendline is good and distributions are roughly symmetric. Since, each CS record represents a possible real earthquake scenario, the isolator is stressed in a variety of ways by different records, leading to a broad distribution of max. displacements. Prior research has demonstrated that CS-based ground motion selection typically results in lower median structural demands compared UHS-based selection. Nevertheless, as here the focus was on the base isolator response itself, the impact on the superstructure subjected to the CS-based approach cannot be demonstrated here. But the spectral acceleration-based fitting seems to bias the displacement-sensitive base isolator. The mean/median isolator displacements at low intensities were highest compared to other method indicating increase in conservative bias. At higher intensities, mean/median isolator displacements closely aligned with those obtained from the spectral matching approach as shown in Figure 5a.

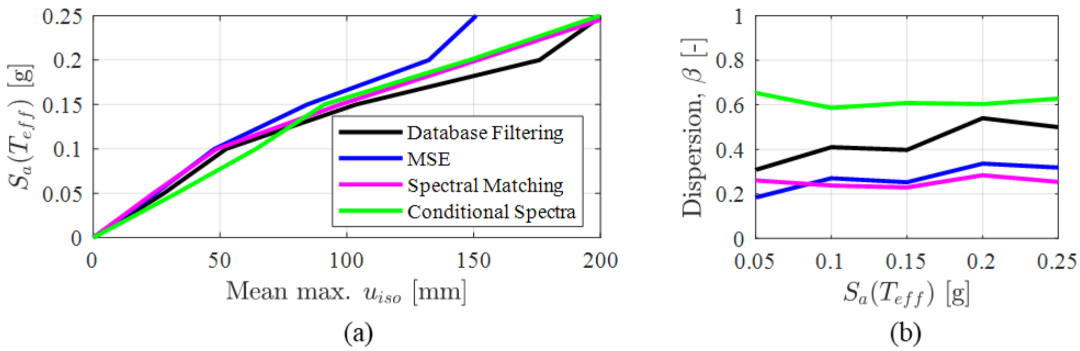

Figure 5. Comparison of (a) Mean isolator displacements trend and (b) dispersion values with increasing intensity level of different ground motion selection procedure

In reference to isolator displacement demands, the *database filtering approach* resulted in the largest mean values and included significant outliers, with displacements even reaching 400–500 mm at RP2500y (Figure 4a), indicating a highly conservative design basis. This was expected but it helps to quantify the relative differences among each other. In contrast, the *Minimize MSE method* consistently produced the lowest mean isolator displacements across all intensity levels (Figure 5a) accompanied by the relatively low dispersion (Figure 5b), making it an efficient selection method for isolator design albeit lacking representation of true hazard variability. The *spectral matching approach* yielded mean displacement values intermediate between those of database filtering and MSE (Figure 5a). Also, a near linear trend in this method of the mean isolator response suggests a design efficiency of isolators. However, its suppressed record-to-record variability underrepresent actual response uncertainty when not adding it back in for design. Finally, the *conditional spectra method* produced larger mean isolator displacements at lower intensity levels, but aligned closely with spectral matching at higher intensities (Figure 5a). It also captured record-to-record variability (hazard-consistent), yet variable perspective on isolator response.

INTERPRETATION AND RECOMMENDATIONS

Why hazard-consistent Conditional Spectra yielded high variability?

The high dispersion from the CS method is a direct consequence of its hazard consistency. In base-isolated systems, isolator displacement demand is influenced by parts of the input spectrum beyond just a single period. A hazard-consistent suite will inevitably contain some records that, although they have the same $S_a(T_{eff})$ at the conditioning period, have more energy in other frequency ranges or longer significant durations, etc., compared to others in the suite. These differences lead to variability in how the isolator responds. In contrast, a spectral matching suite removes most of these differences, artificially yielding low variability in response. Thus, the CS method as strength represents realistic ground motion randomness but its weakness is producing stable and predictable response estimates. Baker (2011) argues that using records that all look like the smooth design spectrum would underestimate the true dispersion in demand. Consequently, CS gives a more realistic picture of uncertainty at the cost of larger scatter in results for the base isolator that engineers must account for (e.g., by designing to a higher percentile of demand rather than the mean or median). Nevertheless, the real benefit of the CS method becomes visible when evaluating the structural response of a base isolated structure which has multiple eigenfrequencies, as on average the applied response spectral values are lower than the target and thus yield into a less severe excitation for the design of the superstructure at the other periods.

Influence of isolator nonlinearity

For base-isolated structures, the isolator period is often well-defined, which naturally draws engineers toward using a fixed conditioning period in CS-based selection. A critical factor is that the isolation system is highly nonlinear and often velocity-sensitive. The period that truly governs isolator displacement is not fixed as it can vary with the hysteretic behaviour. By conditioning on a single spectral acceleration value, the CS method emphasizes matching hazard at that period but does not guarantee accuracy at other periods. For base-isolated structures, other periods (or the overall spectral shape) can significantly influence isolator displacement. Conditioning on an acceleration response spectrum implicitly biases the selection towards matching acceleration amplitudes. Although spectral velocity S_v and spectral displacement S_d are inherently also conditioned using CS-based selection, the modified relative input equivalent velocity spectrum might be more directly tied to large displacements or long-period structures (Mollaioli at el. 2013). The challenge with such intensity measures (IM) lies in their current incompatibility with hazard-consistent computation frameworks.

Recommendations

- Conditioning on a period range ($AvgSa$): Recent research has extended the conditional spectrum concept to such multi-period intensity measures. Kohrangi et al. (2017) introduced a conditional approach using $AvgSa$ as the conditioning IM, effectively conditioning on the spectral shape over a range rather than a single point. The records are selected to collectively match a target spectrum in a broader sense average spectral content over the band of interest, not just at one frequency (O' Reilly 2020). In case of isolators, a band around the effective isolator period (1.5 to 3.5 seconds) might be chosen to capture various spectral contents.

- Use of velocity-based IM: Because base isolators respond strongly to ground velocity and displacement pulses, IM that capture the velocity content of ground motion can be more predictive of isolator demand such as peak ground velocity (PGV) or *AvgSv* - analogous to *AvgSa* but using spectral velocity (pseudo-velocity) over a period range – as an IM.

Based on the study, Table 4 presents a comparative overview of four ground motion selection procedures, ranked by their suitability for seismic isolation design. The ranking is based on subjective engineering judgment and does not represent an absolute guidance in terms of code conformity. It is also acknowledged that the combination of isolator parameters adopted in this study results in a configuration that deviates from conventional design practices. However, the primary objective of this work is to demonstrate a general methodology that remains applicable to other types of isolators, with a particular focus on showcasing the effects of different ground motions on the seismic response.

Table 4: Comparison of ground motion selection procedures for seismic isolation design, highlighting their rank, application context, advantages, disadvantages, and rationale for use.

Selection Procedure	**Rank**	**Use**	**Advantage**	**Disadvantage**	**Rationale**
Spectral Matching	1	efficient and consistent design applications	very low dispersion; highly predictable and smooth median trends;	underrepresent natural ground motion variability; possibly non-conservative if the target is not hazard-consistent	ideal when design confidence and low variability are prioritized (e.g., code compliance, sizing of isolator displacement capacity)
Minimize MSE	2	balance between realism and consistency	low-to-moderate dispersion; preserves real records; matches the target spectrum on average.	does not capture true hazard-based spectral variability; can be biased depending on the target.	provides a practical middle ground-slightly more realistic than spectral matching while still maintaining good response stability
Conditional Spectra	3*	probabilistic risk assessments; hazard-consistent evaluations	hazard-consistent; captures true record-to-record variability; suitable for fragility and uncertainty analysis.	highest dispersion; conditioning period instability for nonlinear isolators; less efficient for design of isolator unless improved (e.g., *AvgSa*, velocity-based conditioning).	robust and appropriate for risk-informed design; however, for nonlinear isolators, single-period conditioning leads to unstable predictions, and dispersion may hinder deterministic design unless properly addressed.
Database Filtering	4	exploratory studies, envelope testing, or conservative checks	simple to implement; wide variability can capture edge-case scenarios.	high dispersion; inconsistent mean trends; not hazard-consistent; possible bias.	useful in preliminary or exploratory stages, but not suitable for detailed design due to its unpredictability and lack of control over spectral compatibility

*If risk-informed design or fragility assessment is the objective, *Conditional Spectra* (with improvements like AvgSa or velocity-based IMs) should increase the ranking. However, if the goal is efficient and reliable design for isolator displacement capacity, *Spectral Matching* currently offers the most stable and conservative basis as long as its limitations are acknowledged.

CONCLUSION

The study systematically evaluated four ground motion selection procedures - database filtering, minimize MSE, spectral matching, and conditional spectra in the context of predicting maximum isolator displacement in a nonlinear base-isolated system. The results demonstrated that the choice of selection method significantly influences both the central tendency and dispersion of isolator responses across intensity levels. Spectral matching emerged as the most effective approach for efficient and consistent design applications, offering minimal dispersion and smooth, predictable response trends. The Minimize MSE method provided a practical compromise between realism and stability. Although the conditional spectra method was the only hazard-consistent technique, it yielded the highest dispersion, primarily due to the instability of the conditioning period in nonlinear systems and its sensitivity to velocity-driven behaviour. The findings underscore the necessity of tailoring ground motion selection to the safety objectives of nuclear installations - whether prioritizing robustness in design or realism in risk quantification - while recommending extensions such as *AvgSa* and velocity-based intensity measures to better align seismic isolation performance with nuclear safety goals. Future research will extend this work by incorporating the dynamic response of the superstructure to provide a more comprehensive understanding of overall system behaviour on ground motion selection.

REFERENCES

Al Atik, L., & Abrahamson, N. (2010). "An improved method for nonstationary spectral matching," *Earthquake spectra*, *26*(3), 601-617.

Ancheta, T. D., Darragh, R. B., Stewart, J. P., Seyhan, E., Silva, W. J., Chiou, B. S. J., ... & Donahue, J. L. (2014). "NGA-West2 database," *Earthquake Spectra*, *30*(3), 989-1005.

Ansys, Inc. (2025). LS-DYNA (2021 R2) [Computer software].

Bassman, T. J., Zhong, K., and Baker, J. W. (2022). "Evaluation of conditional mean spectra code criteria for ground motion selection,", Journal of Structural Engineering, ASCE, 148(11), 04022177.

Baker, J. W. (2011). "Conditional mean spectrum: Tool for ground-motion selection," *Journal of structural engineering*, *137*(3), 322-331.

Baker, J. W., & Lee, C. (2018). An improved algorithm for selecting ground motions to match a conditional spectrum. *Journal of Earthquake Engineering*, *22*(4), 708-723.

Danciu L., Nandan S., Reyes C., Basili R., Weatherill G., Beauval C., Rovida A., Vilanova S., Sesetyan K., Bard P-Y., Cotton F., Wiemer S., Giardini D. (2021). "The 2020 update of the European Seismic Hazard Model: Model Overview," EFEHR Technical Report 001, v1.0.0

Dicleli, M. (2006). "Performance of seismic-isolated bridges in relation to near-fault ground-motion and isolator characteristics," *Earthquake Spectra*, *22*(4), 887-907.

European Committee for Standardization. (2018). "Anti-seismic devices," *EN15129:2018*, Brussels.

IAEA (2020). "Seismic Isolation Systems for Nuclear Installations,", International Atomic Energy Agency, IAEA, IAEA-TECDOC-1905.

Lilhanand, K., & Tseng, W. S. (1988, August). "Development and application of realistic earthquake time histories compatible with multiple-damping design spectra," In *Proceedings of the 9th world conference on earthquake engineering* (Vol. 2, pp. 819-824).

Manfredi, V., Masi, A., Özcebe, A. G., Paolucci, R., & Smerzini, C. (2022). "Selection and spectral matching of recorded ground motions for seismic fragility analyses," *Bulletin of Earthquake Engineering*, *20*(10), 4961-4987.

MATLAB. (2023) "MATLAB2023b," [Computer software], Natick, Massachusetts: The Mathworks Inc.

Mollaioli, F., Lucchini, A., Cheng, Y., & Monti, G. (2013). "Intensity measures for the seismic response prediction of base-isolated buildings," *Bulletin of Earthquake Engineering*, *11*, 1841-1866.

O'Reilly, G. J. (2021). "Limitations of Sa (T1) as an intensity measure when assessing non-ductile infilled RC frame structures," *Bulletin of Earthquake Engineering*, *19*(6), 2389-2417.

Park, Y. J., Wen, Y. K., & Ang, A. H. S. (1986). "Random vibration of hysteretic systems under bi-directional ground motions," *Earthquake Engineering & Structural Dynamics*, *14*(4), 543-557.

Seismosoft. (2020) "SeismoMatch 2025 – Earthquake Software for Response Spectrum Matching," [Computer software].

Wen, Y. K. (1976). "Method for random vibration of hysteretic systems," *Journal of the engineering mechanics division*, *102*(2), 249-263.

Yaacoub, E., Nascimbene, R., Furinghetti, M., & Pavese, A. (2025). "Evaluating Seismic Isolation Design: Simplified Linear Methods vs. Nonlinear Time-History Analysis," Designs, 9(2), 34.